ENERGY-EFFICIENT LTE/WI-FI COEXISTENCE IN THE UNLICENSED SPECTRUM

by

Xiao Han

A Thesis Submitted to the Faculty of the

DEPARTMENT OF ELECTRICAL AND COMPUTER ENGINEERING

In Partial Fulfillment of the Requirements

For the Degree of

MASTER OF SCIENCE

In the Graduate College

THE UNIVERSITY OF ARIZONA

2 0 1 9

THE UNIVERSITY OF ARIZONA
GRADUATE COLLEGE

As members of the Master's Committee, we certify that we have read the thesis prepared by *Xiao Han*, titled *Energy-Efficient LTE/Wi-Fi Coexistence in the Unlicensed Spectrum* and recommend that it be accepted as fulfilling the thesis requirement for the Master's Degree.

Dr. Loukas Lazos — Date: 05/07/2019

Dr. Ming Li — Date: 05/07/2019

Dr. Ravi Tandon — Date: 05/07/2019

Final approval and acceptance of this thesis is contingent upon the candidate's submission of the final copies of the thesis to the Graduate College.

I hereby certify that I have read this thesis prepared under my direction and recommend that it be accepted as fulfilling the Master's requirement.

Dr. Loukas Lazos — Date: 05/07/2019
Master's Thesis Committee Chair
Department of Electrical and Computer Engineering

ACKNOWLEDGEMENTS

First and foremost, I would like to sincerely express my thanks to my academic advisor Dr. Loukas Lazos who has supported me throughout my thesis with his patience and knowledge while allowing me the room to work in my own way. Your passion for your work encouraged me to pursue my own goals, while your attention to detail instilled in me a unique perspective with which to approach problems. I'm fortunate to have you as my advisor. This thesis would have been impossible without your guidance.

I would like to thank Dr. Ming Li and Dr. Ravi Tandon for both supporting my degree goals as well as being my instructors in classes and my thesis defense. Your time and effort are greatly appreciated.

I would like to thank my labmates and colleagues for their help and friendship, including Li Li, Islam Samy, and Nirnimesh Ghose. I would also thank Tami Whelan for handling all the paperwork and giving various forms of support during my graduate study.

I would also like to thank my family and friends for supporting me all this time.

TABLE OF CONTENTS

TABLE OF CONTENTS – *Continued*

LIST OF FIGURES

LIST OF FIGURES – *Continued*

LIST OF TABLES

ABSTRACT

The dramatic growth in demand for wireless services has fueled a severe shortage in RF spectrum, especially in the overcrowded licensed bands. The regulatory approach for meeting this galloping demand is to allow the coexistence of competing wireless technologies (e.g., LTE Unlicensed and Wi-Fi coexisting in the 5GHz U-NII band). This shared spectrum paradigm poses novel challenges for secure, efficient, and fair resource access. Many of these challenges stem from the heterogeneity of the coexisting systems, the system scale, and the lack of explicit coordination mechanisms between them. The fundamentally different spectrum access mechanisms and PHY-layer capabilities–dynamic vs. fixed access, schedule-based vs. random access, interference-avoiding vs. interference-mitigating, etc.–create a complex and interdependent ecosystem, without a unified control plane

Motivated by the shared spectrum paradigm, we address the problem of implicit coordination between coexisting wireless systems that do not share a common control plane. We consider the coexistence of LTE and Wi-Fi and study mechanisms for conserving energy when the wireless channel is occupied. In a Wi-Fi only system, the network allocation vector (NAV) included in the preamble of IEEE 802.11 frames, advertises the duration of an eminent transmission. Nearby Wi-Fi terminals decode the frame preamble and transition to sleep mode to conserve energy. However, when heterogeneous systems co-exist (e.g., LTE and Wi-Fi), frames that belong to other systems are not decodable, leading to continuous channel sensing, even when the channel is to be occupied for long duration.

In this thesis, we study mechanisms to achieve coordination between LTE and Wi-Fi operating on the same band, without relying on explicit messaging. We develop and implement several implicit techniques for monitoring the operational

parameters of LTE on Wi-Fi side. We use these parameters to conserve energy at Wi-Fi terminals by transitioning them to sleep mode whenever the channel is occupied by an LTE station. We exploit the unique backoff characteristics of each priority traffic class to predict the length of an imminent LTE transmission. We propose two class estimation mechanisms. The first is a conservative mechanism that maximizes the Wi-Fi sleep time without missing an opportunity to contend for the channel. In the second mechanism, we apply Bayesian estimation to get a more accurate prediction of the priority class and avoid waking up the receiver too early. This comes at the expense of oversleeping when a high priority class is misclassified, thus leading to a small loss in transmission opportunities. Although we present our work from the Wi-Fi perspective, the same methodology can be applied to conserve energy on the LTE side.

CHAPTER 1

INTRODUCTION

1.1 Motivation and Scope

The ever-increasing demand for wireless services has led to an exponential increase in mobile data traffic and a severe shortage in the radio spectrum in the overcrowded licensed bands. One promising approach to address the spectrum scarcity is to allow offloading of network traffic to unlicensed bands, leading to the coexistence of heterogeneous wireless systems [1–4]. As an example, the long term evolution (LTE) unlicensed standards regulate the co-existence of LTE stations with Wi-Fi terminals in the 5GHz unlicensed band. Two main LTE standards variants are been promoted: LTE-U and LTE-LAA. The former standard implements a duty cycle approach based on Carrier-Sensing Adaptive Transmission (CSAT) mechanism introduced by Qualcomm [5]. The LTE-LAA standard implements a Listen-Before-Talk (LBT) mechanism that coordinates channel access based on channel sensing [6]. The latter has been promoted in recent LTE standards, e.g. LTE release 15 [6], as it allows fairer spectrum allocation.

The main challenge in achieving a fair and efficient co-existence between heterogeneous systems is the lack of a common control plane. Without explicit coordination messages, terminals rely on channel sensing to infer the channel state (idle or busy) and access the channel. For instance, consider the co-existence of two LTE stations A and B with three Wi-Fi terminals C, D, and E, as shown in Figure. 1.1. Let C capture the channel first by following the backoff mechanism of IEEE 802.11. The Wi-Fi terminal defers for DIFS time, followed by a backoff, followed by a data transmission and an ACK response from receiver D. The preamble of the data frame contains a network allocation vector (NAV) field that advertises the duration

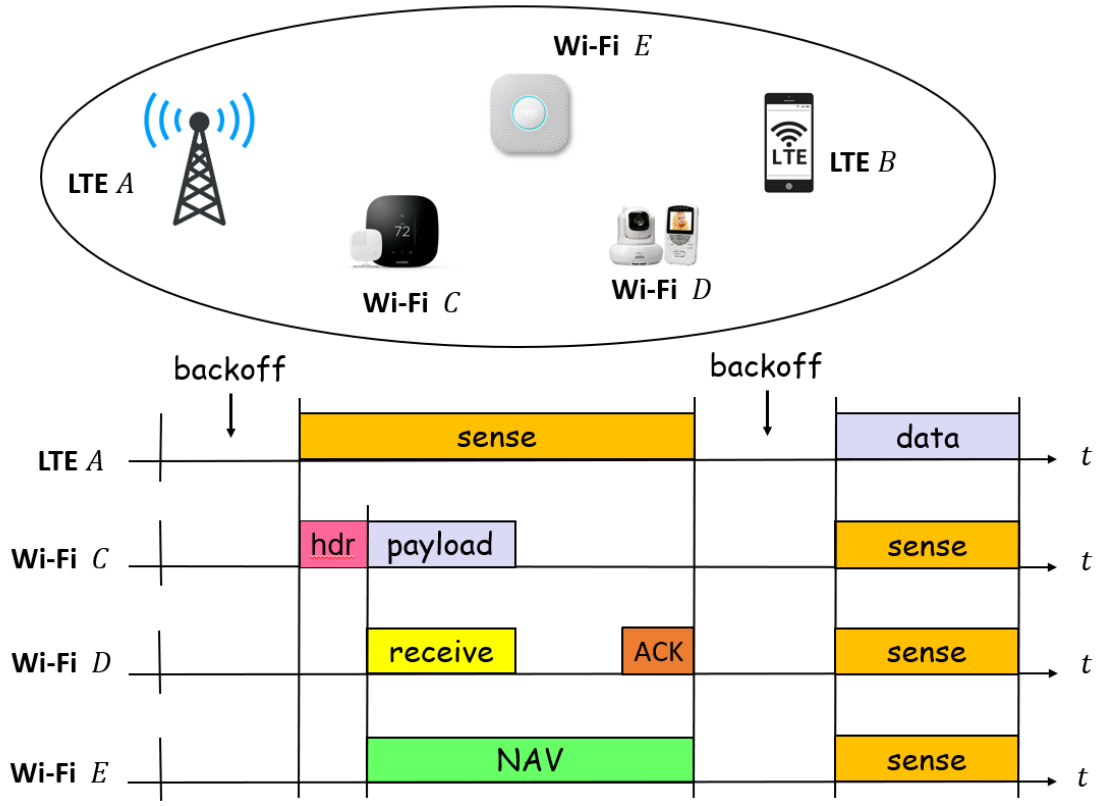

Figure 1.1: LAA-LTE/Wi-Fi Coexistence.

of the Wi-Fi transmission. All neighboring Wi-Fi terminals decode the preamble to determine the frame destination. If a terminal is not the destination like terminal E, it uses the NAV to switch its receiver to a sleep state and conserve energy.

However, when A is transmitting to B, the co-existing Wi-Fi stations do not decode the LTE frame. As a result, they have no way to determine the duration of the LTE transmission and stay in idle mode, continuously sensing the channel to be able to contend once the channel is freed. This leads to unnecessary power consumption with every LTE transmission. The same phenomenon occurs when the LTE station overhears a Wi-Fi transmission, as it has no way to a priori determine the duration of the Wi-Fi transmission. We emphasize that the energy consumption during the idle sensing state is several orders of magnitude higher than that of the sleep state. To conserve energy, we study the problem of estimating the transmission

duration of LTE stations at the beginning of each transmission, with the purpose of setting the Wi-Fi receiver to sleep mode. A requirement is that the estimation is performed implicitly, without decoding LTE transmissions or signaling over a common control channel.

1.2 Main Contribution and Thesis Organization

We address the problem of conserving the energy under the LTE/Wi-Fi coexistence paradigm. We develop and implement several techniques for monitoring the operational parameters of LTE, without relying on explicit messaging. First, we adopt cyclic-prefix (CP)-based method proposed in [7]. Then, we adopted the mechanism proposed by [8] to differentiate between LTE stations by correlating the unique physical layer identity of an LTE station. We also adopted the mechanism to identify the retransmission round r. In addition, we evaluated these techniques using experimental setup and verified their accuracy in practical scenarios. Hence, we use these parameters to conserve energy at Wi-Fi terminals by transitioning them to sleep mode whenever the channel is occupied by an LTE station. We exploit the unique backoff characteristics of each priority traffic class to predict the length of an imminent LTE transmission. We propose two class estimation mechanisms. The first is a conservative mechanism that maximizes the Wi-Fi sleep time without missing any opportunity to contend for the channel. In the second mechanism, we apply Bayesian estimation to get a more accurate prediction of the priority class and avoid waking up the receiver too early. This comes at the expense of oversleeping when a high priority class is misclassified, thus leading to loss of transmission opportunities. Our simulations show that the first approach reduces energy consumption by 70% with zero oversleeping probability, whereas the second approach conserves up to 85% energy, at the expense of a small loss in transmission opportunities. Although we present our work from the Wi-Fi perspective, the same methodology can be applied to conserve energy at the LTE side.

The remainder of this thesis is organized as follows. The background and re-

lated works are discussed in Chapter 2. Chapter 3 introduces the system model and overviews the proposed power-saving mechanisms. The adopted implicit sensing mechanism for estimating the elapsed idle slots and the experiment results for detecting LTE transmissions are detailed in Chapter 4. In Chapter 5, we discuss the idle slots estimation and two proposed priority class estimation schemes. We evaluate the performance of proposed power-saving mechanisms in Chapter 6. We summarize the main contributions of this thesis in Chapter 7.

CHAPTER 2

BACKGROUND AND RELATED WORK

In this chapter, we introduce relevant background and the related works. In Section 2.1, we outline the Wi-Fi power management. In Section 2.3 and Section **??**, we discuss the LTE-U specification introduced by Qualcomm [5] and the LAA-LTE as described in the 3GPP Release-15 standard [6].

2.1 Wi-Fi Power Management

In IEEE 802.11 family of standards [9], a Wi-Fi terminal supports several power-management modes. Each mode is a combination of device activity and network connectivity. The power-management modes are described below.

1. Active: the Wi-Fi terminal is connected to the network and is actively transmitting or receiving.

2. Idle: the Wi-Fi terminal is connected to the network but is not actively transmitting or receiving.

3. Sleep: the Wi-Fi terminal is connected to the network, but the remainder of the platform is in a very low-power state. Wake on pattern match is enabled so that the Wi-Fi terminal wakes the system on a chip (SoC) on a specific set of incoming frames.

4. Disconnected sleep: the Wi-Fi device is not connected to the network and the remainder of the platform is in a very low-power state. Pattern-match wake and the Network Offload list are enabled. The Wi-Fi device implements the Network Offload list to periodically scan the channel.

5. Radio off: the Wi-Fi device has power supply but the radio (RF components) are powered down.

6. Device powered down: the Wi-Fi device has been completely powered down.

Wi-Fi terminals transition between different modes depending on the state of the 802.11 protocol. For this thesis, we are only concerned about the first three modes where the device is in a connected state. When it is involved in a transmission/reception, the terminal is in active mode. If it is monitoring the channel for a transmission opportunity (e.g., during the backoff period), the terminal is in idle mode, whereas it transitions to sleep mode for the period of time that other terminals are active. The sleep time is calculated based on the NAV as shown in Fig. 1.1. The Wi-Fi terminal defers for DIFS time and waits until backoff counter is zero. If the collision happens, Wi-Fi terminal doubles contention window size. After the random channel access process, Wi-Fi terminal sends a data transmission, followed by an ACK response from receiver. The preamble of the data frame contains the network allocation vector (NAV) field that advertises the duration of the Wi-Fi transmission. All neighboring nodes decode the preamble to determine the destination. If a terminal is not the destination, it uses the NAV to switch off its receiver. The power consumption in active mode is about 1.687W while transmitting and 1.585W while receiving. The consumption drops to 1.038W for the idle mode, and only 0.088W for sleep mode [10]. It is evident that setting the terminal to sleep mode when possible can lead to dramatic energy savings.

2.2 LTE-U

LTE-U is the first proposed LTE standard for operating in unlicensed spectrum [5]. It implements a duty cycle approach based on Carrier-Sensing Adaptive Transmission (CSAT) mechanism to ensure the LTE/Wi-Fi coexistence. In countries such as the United States, China, and South Korea, there is no regulatory requirement for "Listen-Before-Talk" (LBT) mechanism for the unlicensed bands. Operators can

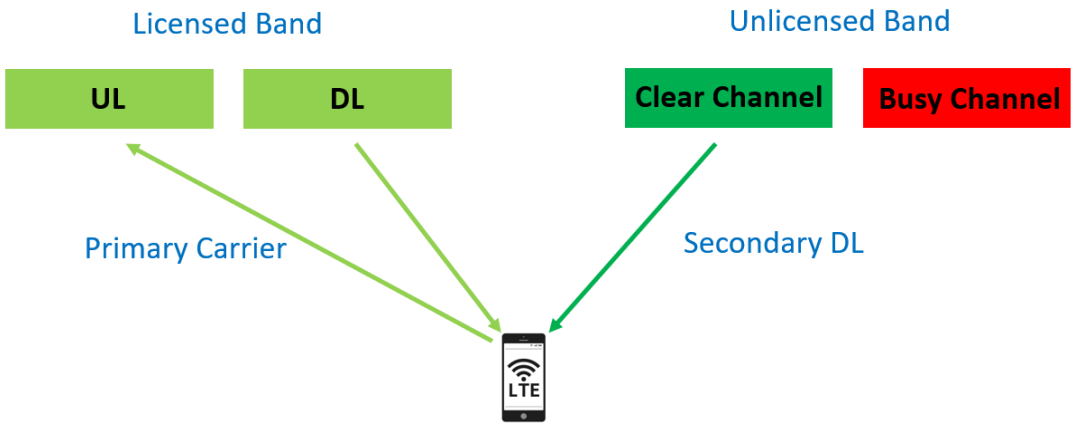

Figure 2.1: Channel selection for LTE-U SDL transmission.

deploy LTE-U in unlicensed bands that are fully compatible with 3GPP Release 10/11 [11, 12] and does not require any changes of LTE specification. It employs carrier aggregation technology introduced in 3GPP Release 10 and allows UEs to aggregate unlicensed carrier (i.e., SDL mode) with a primary carrier in licensed bands so that service reliability can be guaranteed. The coexistence mechanisms used in LTE-U are CSAT and SDL. The channel access mechanism of LTE-U is introduced as follows.

Channel selection: LTE-U small cells scan the unlicensed band and identify the empty channels as SDL carriers as shown in Figure 2.1. If the channel in unlicensed bands is empty at an initial stage, UE sets that channel for SDL carrier transmission and aggregates it with the primary DL carrier. LTE-U periodically measures the interference level at the SDL operation stage by energy detection, which also diagnoses the interference type and number of interference sources. If the operating channel has interference and there is another channel available, the SDL carrier is switched to the new channel using 3GPP Release 10 procedures.

Carrier-sensing adaptive transmission (CSAT): In the hyper-dense deployment of Wi-Fi and LTE-U small cells, there is possible that no empty channel available for LTE-U in unlicensed bands. In this case, LTE-U can coexist with Wi-Fi

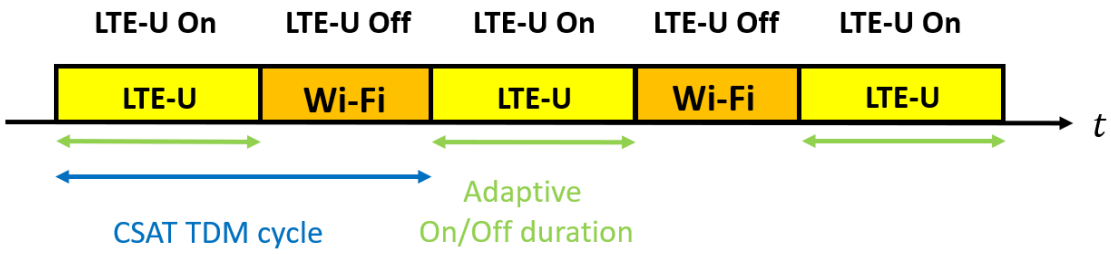

Figure 2.2: CSAT enables LTE-U/Wi-Fi Coexistence.

neighbors by using CSAT mechanism. LTE-U accesses spectrum in a time division multiplexing based fashion as shown in Figure 2.2. Specifically, CSAT defines a time cycle where the small cell transits in a fraction of the cycle and gates off in the remaining cycle. The LTE-U, on the secondary cell, is periodically activated and deactivated. During LTE-U off period, the neighboring Wi-Fi terminals occupy the channel and resume normal transmissions. The LTE-U senses the active Wi-Fi transmissions during LTE-U off period and adjusts its duty cycle accordingly.

Opportunistic SDL: In Figure 2.1, the primary carrier in the licensed band is always available, so the secondary DL is used on an opportunistic base. The SDL is turned on when the DL traffic exceeds a certain threshold and there are active users within the coverage of the unlicensed band, otherwise, SDL is turned off if there are no active users within the coverage of the unlicensed band.

2.3 LAA-LTE Release 15

We consider the LAA-LTE specification as described in the 3GPP Release-15 standard [6]. The LAA-LTE standard defines four traffic priority classes, listed in Table 1. Each class C_ℓ is defined by a three-tuple $(\rho_\ell, T_\ell^{MCOP}, \mathbf{q}_\ell)$ where ρ_ℓ denotes the number of slots an LTE station has to defer before starting the backoff process, T_ℓ^{MCOP} denotes the maximum channel occupancy time, and $\mathbf{q}_\ell$ is the vector of all possible contention window sizes. Priority classes C_1 and C_2 are designed for con-

Figure 2.3: Backoff between two consecutive transmissions.

Table 2.1: Priority Classes in LTE-LAA.

Priority Class	ρ_ℓ	q_{min}	T_ℓ^{MCOP} (ms)	Allowed $\mathbf{q}_\ell$ sizes
C_1	1	4	2	$\{4, 8\}$
C_2	1	8	3	$\{8, 16\}$
C_3	3	16	8 or 10	$\{16, 32, 64\}$
C_4	7	16	8 or 10	$\{16, 32, \ldots, 1024\}$

trol and short duration frames, whereas priority classes C_3 and C_4 are designed for longer, lower-priority data. The channel access mechanism of LAA-LTE is illustrated in Figure 2.3 and described in the following steps:

1. Upon the end a of previous transmission, an LTE station senses the channel for T_{init} which consists of a defer time $T_{def} = 16\mu s$ plus ρ_ℓ observation slots of $T_s = 9\mu s$ each. If the channel stays idle during T_{init}, the LTE station initiates the backoff process. Otherwise, the channel sensing is repeated. The channel is considered idle if the received power is less than the clear channel assessment (CCA) threshold (≈ -73 dBm) for at least $4\mu s$.

2. During the backoff stage, the LTE station uniformly draws a backoff counter N from $[0, q_{\min} - 1]$. The LTE station decrements its backoff counter by one with every idle slot and freezes it on a busy slot. The backoff countdown resumes if the channel is idle for T_{init}.

3. When $N = 0$, the LTE station transmits a frame with maximum duration of T_ℓ^{MCOP} and waits for the ACK. If the ACK is received before a time out, this

transmission round is completed, Otherwise, the process is repeated from step 1 with a doubled CW.

In Table 2.1, we note that the defer slots ρ_ℓ, the contention window size $\mathbf{q}_\ell$, and the maximum transmission duration T_ℓ^{MCOP} differ according to the priority class. Our goal is use these different parameters to implicitly estimate the class of an imminent LTE transmission so that a Wi-Fi terminal can transition to sleep mode during the LTE transmission without losing any future transmission opportunities.

2.4 Related Work

The LTE/Wi-Fi coexistence in unlicensed bands has created new challenges for the fair and efficient resource management [13–15]. Performance and analysis in Ratasuk *et al.* [16] showed that LTE can deliver significant capacity even in heterogeneous systems. Meanwhile, they discussed several modifications that enable LTE to operate in an unlicensed band, and also the LTE/Wi-Fi coexistence mechanisms. However, Sagari *et al.* [13] showed that both LTE and Wi-Fi networks cause significant interference to each other and lead to a great performance degradation due to the absence of a common control plane between LTE and Wi-Fi in the same band. In addition, Wi-Fi and LTE use different channel access mechanisms. For example, Wi-Fi uses random access mechanism, whereas LTE uses schedule based mechanism. To guarantee the fairness between different channel access mechanisms, Cano *et al.* [17] studied the fair coexistence of schedule based and random access mechanisms in the same channel. They showed that there is an inherent cost of throughput/delay due to the heterogeneity of random access mechanisms. In some certain circumstances, the heterogeneity cost of CSAT is higher than Listen-Before-Talk (LBT). To further achieve the fairness in LTE/Wi-Fi coexistence, Hirzallah *et al.* [7] first presented that the different access mechanisms for Wi-Fi and LTE can cause great collision rate and latency for both system, then they adopted Clear Channel Assessment (CCA) threshold adaptation scheme for Wi-Fi system to pro-

mote the fairness and performance between the two systems. Furthermore, recent works have developed implicit methods to estimate the operational parameters of heterogeneous systems that do not require frame decoding [8, 14, 18]. To solve the lack of common control plane between LTE and Wi-Fi, Samy *et al.* [8] proposed a framework that enables the Wi-Fi to implicitly monitor the operational parameters of LTE, which is the fundamental of this thesis. However, non of these papers studied the energy-efficient LTE/Wi-Fi coexistence in unlicensed bands.

Energy-efficient medium access has been a topic of extensive research in homogeneous networks, wireless sensor networks in particular [19–27]. As sensor nodes are generally battery-powered devices, the pivotal aspect to concern is how to reduce the power consumption so that the lifetime of battery can be extended to a reasonable time. The power consumption of sensor nodes can be reduced by applying different techniques. For example, devices aim to reduce power consumption during network activities by implementing energy-efficient protocols. However, a considerable amount of energy is consumed by node components (CPU, radio, etc) even they stay idle. Power management schemes are thus used for temporarily switching off node components when they are not needed. In duty cycling , which is the most effective energy-efficient operation by switching off radio transceiver, power management schemes are further subdivided to two broad categories. The first category is sleep/wakeup protocols and the second one is MAC protocols with low duty-cycle. In this thesis, we mainly focus on the MAC protocols with low duty-cycle, especially, in Time Division Multiple Access (TDMA) protocols and Contention-based MAC protocols.

TDMA protocols [28–30] naturally enable Wi-Fi terminals to access the channel on a slot-by-slot basis. As terminals need to turn on their RF during their own slots to transmit/receive packets, the power consumption is ideally reduced to the minimum requirement of transmitting/receiving. Heinzelman *et al.* [30] proposed the LEACH (Low-Energy Adaptive Clustering Hierarchy), a clustering-based routing protocol that minimizes power consumption by distributing data traffic to each

node at different points in time. In this protocol, Wi-Fi terminals are grouped to form clusters with a cluster-head which takes charge of assigning slots to each node in the cluster. By using localized coordination and data fusion to reduce the total information transmission, LEACH achieved considerable reduction in energy consumption compared with former routing protocols. Moreover, TRAMA, another energy-efficient TDMA protocol for wireless sensor networks is proposed in [29]. TRAMA reduces power consumption by avoiding collisions during unicast and broadcast transmissions, and also by allowing Wi-Fi terminals to switch off to idle state when no transmitting/receiving needed. It assumes time is slotted and the time slots are reserved for active terminals by using distributed election scheme and accessed with a contention-based protocol. TRAMA avoids assigning time slots to terminals with no data to send and allows terminals to switch off to idle mode when terminals are not active. Since the time slot reservation algorithm in these works tend to be complex and not flexible, researchers have been working to simplify the slot assignment and also achieving a good energy efficiency [31, 32].

Contention-based MAC protocols are the most popular class of MAC protocols for wireless sensor networks. Polastre *et al.* [33] proposed B-MAC, a low complexity and low power MAC protocol for wireless sensor network that provides a flexible interface to obtain high performance. It implements a backoff scheme to effectively perform clear channel estimation. Furthermore, to achieve low power operation, it implements an asynchronous sleep/wake scheme based on periodic listening, which is first introduced in [34]. Ye *et al.* [35] proposed S-MAC (Sensor-MAC), a famous MAC protocol enables low-duty-cycle operation for multi-hop sensor networks. It allows terminals to exchange sync packets for coordination among terminals and collision avoidance. Thus, terminals form a virtual cluster based on the common sleep schedules and enable traffic-adaptive wake-up. However, even though duty-cycle based protocols are energy-efficient, the terminals have to wait until the receiver wakes up, then the terminals are able to send the packets. This latency increases with the number of terminals in the same locality. Moreover, the duty cycle based solutions proposed for wireless sensor networks are not suitable for high traffic sce-

narios. Meanwhile, periodic wakeups are not throughput-effective under saturation conditions studied in this work.

CHAPTER 3

SYSTEM MODEL AND OVERVIEW

In this chapter, we introduce the system model and provide an overview of the proposed power-saving mechanisms.

3.1 System Model

We consider the coexistence of an LAA-LTE system with a set of 802.11ac Wi-Fi terminals in the 5GHz unlicensed band. All stations are assumed to be in the same collision domain and operate under backlogged traffic conditions. The power consumption of Wi-Fi terminals in active, idle, and sleep modes are denoted by P_A, P_I and P_S, respectively, and is assumed to be constant while the terminal is in any of these modes. The LTE and Wi-Fi terminals do not decode the transmissions from other systems. However, they still have the opportunity to sample the received signals from other technologies. There is no centralized control or a common control plane between the two systems. A central node may exist to coordinate various network function within each system.

Problem statement: Consider a Wi-Fi terminal X operating over a period of time T. The total energy E_T consumed by X in T is given by

$$E_T = P_A \cdot T_A + P_I \cdot T_I + P_S \cdot T_S, \tag{3.1}$$

where T_A, T_I, and T_S are the times spent in active mode, idle mode, and the sleep mode, respectively, with $T_A + T_I + T_S = T$. To conserve energy at X, we wish to minimize E_T, without reducing the time spent in active mode, which is used for useful communications. As $P_I >> P_S$, by making sure to transition to sleep mode

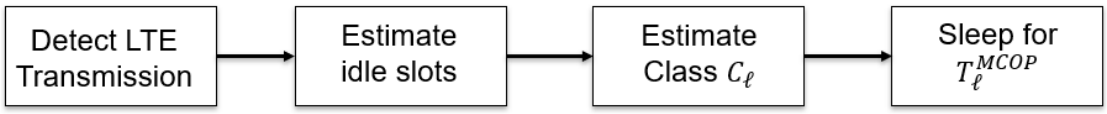

Figure 3.1: Steps for transitioning to sleep mode.

each time the channel is busy, taking into account avoiding oversleeping under the idle channel conditions, the energy minimization problem becomes equivalent to maximizing T_S or minimizing T_I. To achieve that, once the Wi-Fi terminal experiences a busy channel, it decides to sleep until the channel is idle again. For an LTE transmission, the AP identifies that duration by inferring the used priority class. Given an estimated priority class $C_\ell^\star$, the saved energy E_S is determined as follows,

$$E_S = P_I \cdot T_\ell^{MCOP} - P_S \cdot T_{\ell^\star}^{MCOP}, \tag{3.2}$$

$T_{\ell^\star}^{MCOP}$ and T_ℓ^{MCOP} are the frame duration of the estimated class $C_\ell^\star$ and the true class C_ℓ of the transmitted frame. In this thesis, we show how the monitoring Wi-Fi terminals infer the priority class at the beginning of LTE transmissions.

3.2 Proposed Power-saving Mechanisms

To minimize the power consumption, we propose implicit mechanisms that enable Wi-Fi terminals recognize opportunities to transition from idle mode to sleep mode. The ideal solution would allow the Wi-Fi terminal to sleep for T_ℓ^{MCOP} when an LTE transmits a frame of class C_ℓ. The duration T_ℓ^{MCOP} can be easily predicted from Table 2.1, if the class C_ℓ of a transmitted frame is predicted. However, this posses several challenges because LTE frames are undecodable by Wi-Fi terminals. We propose to *implicitly estimate* the class of an imminent LTE transmission using protocol semantics and prior history.

Our mechanisms consist of the steps shown in Figure. 3.1. Initially, a Wi-Fi

terminal X monitors the channel and counts the elapsed idle slots between two consecutive transmissions attributed to the same LTE station. The number of idle slots is use to estimate the priority class. This estimation is done using two approaches. The first approach is a conservative one where X assumes the minimum T_ℓ^{MCOP} possible given the inferred protocol parameters (ρ_ℓ and $\mathbf{q}_\ell$). This guarantees that X will not miss a transmission opportunity by oversleeping (still being in sleep mode while the LTE transmission has finished), but can lead to higher energy consumption because X tends to wake up too early. In the second approach, we apply Bayesian estimation to accurately estimate the priority class, at the expense of a non-zero oversleeping probability. The proposed power-saving mechanisms can be summarized as follows:

1. During each backoff period, Wi-Fi terminal X estimates the number of idle slots.

2. Wi-Fi X compare the number of idle slots with the expected range of idle slots if priority class C_ℓ is used. If the number of idle slots lies in the expected range, priority class C_ℓ is possible class and under the consideration of Wi-Fi AP. Otherwise, C_ℓ is excluded by Wi-Fi AP.

3. For the first approach, Wi-Fi X maximizes the sleeping time without missing any possible transmission opportunities caused by oversleeping.

4. For the second approach, given the estimated number of idle slots and the observed history, Wi-Fi X applies the Bayesian estimation to estimate the most probable priority class and sleep for the corresponding frame duration T_ℓ^{MCOP}.

CHAPTER 4

DETECTING LTE TRANSMISSIONS

In this chapter, we discuss the framework for implicitly inferring different parameters of LTE transmissions on Wi-Fi side. Specifically, We introduce three implicit mechanisms that enable Wi-Fi terminals to detect LTE signals, differentiate LTE transmissions, and identify the transmission round. We further study the accuracy of the proposed implicit techniques through experimentation.

4.1 Identifying LTE Signals

The first step for estimating the idle slots is to determine when LTE stations access the wireless medium. To detect LTE transmissions, we adopt the cyclic prefix (CP)-based method proposed in [36]. Briefly, the CP detection operates as follows. LTE transmissions, like any other OFDM modulated signal, utilize the CP concept to mitigate inter-symbol interference (ISI) between two consecutive symbols. The CP is a replication of the end of an OFDM symbol, copied at the beginning of that symbol, as shown in Figure. 4.1.

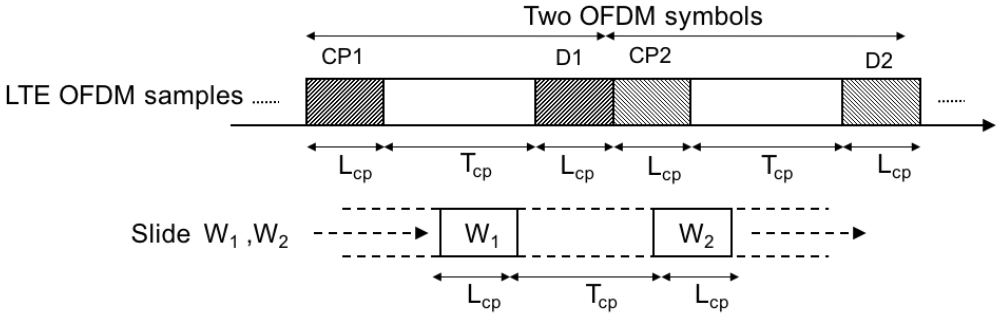

Figure 4.1: Detecting LTE transmissions using CP.

Let L denote the length of the CP in samples and N denote the length of an OFDM symbol in samples. Parameters L and N are fixed to unique values in the LTE standard [6]. A Wi-Fi terminal that cannot decode an LTE transmission can try to detect it by estimating parameters L and N via signal sampling and signal correlation.

A Wi-Fi terminal first samples the received signal and stores the samples. It fixes two time windows W_1 and W_2 of length L, separated by $N-L$ samples. Then, it shifts the two windows simultaneously by one sample at the time while keeping the window separation fixed to $N-L$. For each shift n, Wi-Fi terminal obtains the corresponding received signal samples $s_1(n)$ and $s_2(n)$ and computes a correlation timing metric $\rho(n)$ as

$$\rho(n) = \frac{|A(n)|^2}{(\max(E_{s_1}(n), E_{s_2}(n)))^2}, \tag{4.1}$$

where $A(n)$ is the correlation between $s_1(n)$ and $s_2(n)$, calculated as

$$A(n) = \sum_{k=0}^{L-1} s_1(n-k)s_2^*(n-k-N). \tag{4.2}$$

Whereas, $E_{s_1}(n)$ and $E_{s_2}(n)$ are the energies of $s_1(n)$ and $s_2(n)$, respectively, written as

$$E_{s_1}(n) = \sum_{k=0}^{L-1} s_1(n-k)s_1^*(n-k), \tag{4.3}$$

$$E_{s_2}(n) = \sum_{k=0}^{L-1} s_2(n-k-N)s_2^*(n-k-N). \tag{4.4}$$

where s_1^* and s_2^* is the complex conjugate of s_1 and s_2, respectively. If $s_1 = s_2$, the correlation spikes relatively to the case of $s_1 \neq s_2$ indicating that s_1 is the CP of s_2 and that s_2 occurs $N-L$ samples away, thus confirming the LTE OFDM symbol structure. This also allows Wi-Fi terminals to synchronize with the start of the LTE frame and determine the starting time $t_s(i)$ and end time $t_e(i)$.

4.2 Differentiating Between LTE Stations

Although the CP-based detection approach can identify LTE transmissions without decoding, it cannot attribute transmissions to individual LTE stations. This is necessary for estimating the number of idle slots between two successive transmissions from the same station. In an LTE system, an LTE transmission carries the station identity ID_j which is calculated as $ID_1 + 3ID_2$, where ID_1 and ID_2 define the physical-layer cell identity group and physical layer identity, respectively. The ID_1 and ID_2 fields are part of the primary synchronization signal (PSS) and secondary synchronization signal (SSS), respectively. The pair (ID_1, ID_2), which defines ID_{cell}, is unique for every LTE station, however they can only be obtained if the PSS and SSS are decoded. As shown in Figure. 4.2, the PSS and SSS fields appear at fixed locations in an LTE frame and also have a fixed duration in number of OFDM symbols or signal samples. Monitoring Wi-Fi terminals can exploit the known LTE frame structure to attribute LTE transmissions to different LTE stations. Note that we are not interested in extracting ID_j, but in attributing LTE transmissions to unique LTE stations to estimate the number of idle slots between two successive transmissions. This is achieved by exploiting the same signal correlation principle used to identify LTE transmissions. The main idea is to detect the unique header fields (ID_1, ID_2) by sampling the LTE transmission at the PSS and SSS locations and correlating the signal samples with previously recorded samples. Two transmissions from the same LTE station will exhibit high correlation on the ID fields. Note that the IDs themselves are not decoded, because correlation of the sampled values suffices for classification purposes. A monitoring Wi-Fi terminal executes the following LTE transmission classification algorithm.

Step 1: The Wi-Fi terminal applies the CP-based LTE detection method to identify the i^{th} LTE transmission and synchronizes with the start time $t_s(i)$.

Step 2: The Wi-Fi terminal extracts the samples $s_{ID}^{(i)}$, of length L_{ID}, that correspond to ID_1 and ID_2 in the PSS and SSS fields, respectively (the two fields

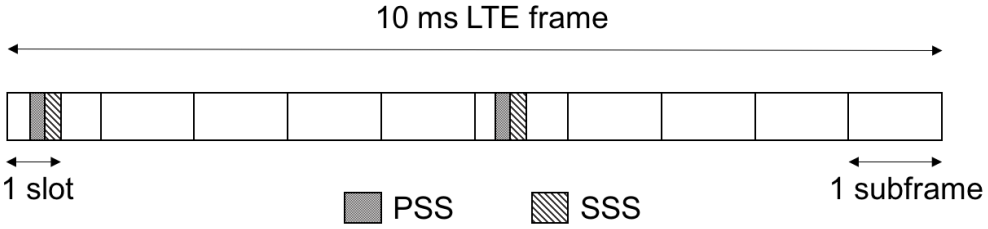

Figure 4.2: The PSS ans SSS fields in LTE frames.

are contiguous).

Step 3: The Wi-Fi terminal maintains a signature database for all LTE stations. The signature of the j^{th} LTE is the sampled form s_{ID_j} of $ID_1||ID_2$. For the i^{th} LTE transmission, the Wi-Fi terminal computes the signal correlation as follows,

$$\rho_{ID}^{(i,j)} = \frac{|\sum_{k=1}^{L_{ID}} s_{ID_j}^{*}(k)\ s_{ID}^{(i)}(k)|^2}{(\max(E_{s_{ID_j}}, E_{s_{ID}^{(i)}}))^2}, \forall j, \tag{4.5}$$

where $E_{s_{ID_j}}$ and $E_{s_{ID}^{(i)}}$ are the energies of the samples in s_{ID_j} and $s_{ID}^{(i)}$, respectively, calculated in a similar way to (4.3) and (4.4).

Step 4: The Wi-Fi terminal attributes the i^{th} LTE transmission to LTE j that yields the maximum $\rho_{ID}^{(i,j)}$, given that $\rho_{ID}^{(i,j)} \geq \gamma_0$. Here γ_0 is a minimum correlation threshold that defines a signal match. If a match is found, the Wi-Fi terminal also replaces the current signature of LTE j with $s_{ID}^{(i)}$.

Step 5: If no correlation value exceeds γ_0, the Wi-Fi terminal adds $s_{ID}^{(i)}$ as a new LTE station signature to the database.

The correlation-based classification method presents challenges when LTE transmissions collide (with other LTE or with Wi-Fi). However, performing classification via signal cancellation in the presence of collisions is possible as shown in [37].

4.3 Identifying the Transmission Round

To identify the transmission round, we adopt the correlation-based classification method presented in detecting LTE signals and differentiating LTE stations. We assume that the header of the frame remains the same in each retransmission. So, we evaluate the similarity of headers among frames. The correlation is high, when the frame is a retransmission. The correlation-based classification is performed via signal cancellation as discussed earlier to identify the collisions.

4.4 Experimental Validation of Implicit Techniques

In this section, we study the accuracy of the proposed implicit techniques presented in previous sections through experimentation.

4.4.1 Experimental Setup

We performed all experiments using NI-USRP 2921 devices. We considered one Wi-Fi terminal overhearing the transmissions of one LTE station, each terminal was implemented in an USRP device. The devices were set to work at the 5 GHz band and were synchronized to the clock of a personal computer via a cable. The transmission bandwidths were set to 2.5MHz and 20MHz for LTE and Wi-Fi, respectively, whereas the IQ rate was set to 1.92MHz for both. The LTE frame duration was fixed to 10 ms. Each frame was implemented with 10 subframes with 2 slots for each. Each slot has a duration of 0.5 ms consisting of 6 OFDM symbols. Each OFDM symbol consists of N samples. $N - L$ samples represent the payload, whereas the remaining L samples are related to the extended cyclic prefix. The duration of each OFDM symbol is 83.4μs, 66.7μs for the payload and 16.7 μs for the extended CP. We set up all these physical layer parameters from [38]. The experimental setup is shown in Figure. 4.3.

4.4.2 Detecting LTE Transmissions

In the first set of experiments, we evaluated the Wi-Fi's capability in identifying LTE signals. The identification is performed using the CP-based method proposed in Section 4.1. Parameters N and L are fixed to 320 samples and 64 samples, respectively. We tested two scenarios: (1) Wi-Fi terminal is stacked on top of the LTE, and (2) Wi-Fi terminal is moved away from the LTE. The LTE station adopted the quadrature phase shift keying (QPSK) modulation to transmit OFDM symbols and repeatedly transmitted message {0,1,1,0}. The Van De Beek algorithm [39] was implemented on the Wi-Fi terminal to estimate the carrier frequency offset.

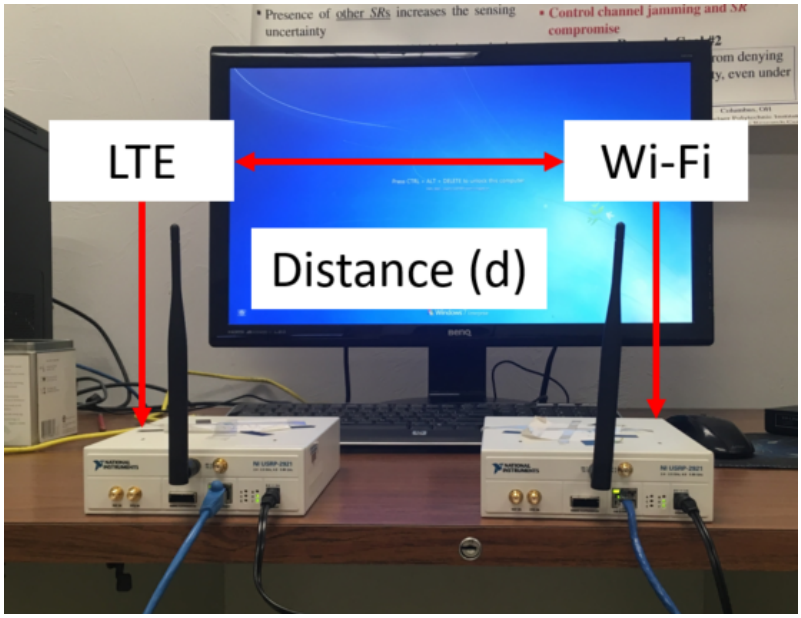

Figure 4.3: Experimental setup.

We calculated the correlation metric $\rho(n)$ using (4.1), as a function of the OFDM symbol index when ten symbols are detected. We repeated the same experiment but reconfigured the USRP device representing the LTE station to transmit Wi-Fi OFDM symbols, each has a 4μs duration (3.2μs for the payload and 0.8μs for the CP). Thus, each symbol was realized with 80 samples including 16 samples for cyclic prefix. We then recalculated the correlation metric $\rho(n)$ for this scenario.

Figure. 4.4 shows $\rho(n)$ as a function of the OFDM symbol index when ten OFDM symbols are transmitted. We observe that when these symbols belong to the LTE station, the correlation peaks and $\rho(n)$ is always higher than 0.6. Whereas, with the same window size $L = 320$ and separation length $N = 64$, the correlation in the case of Wi-Fi OFDM symbols is almost zero. This is because the samples in each of the two windows are expected to be independent of each other when Wi-Fi OFDM symbols are transmitted due to the differences in N and L.

Figure. 4.5(a) show the detection P_d and false alarm P_{fa} probabilities for the CP-based approach. To achieve accurate results, we transmitted 6000 OFDM symbols

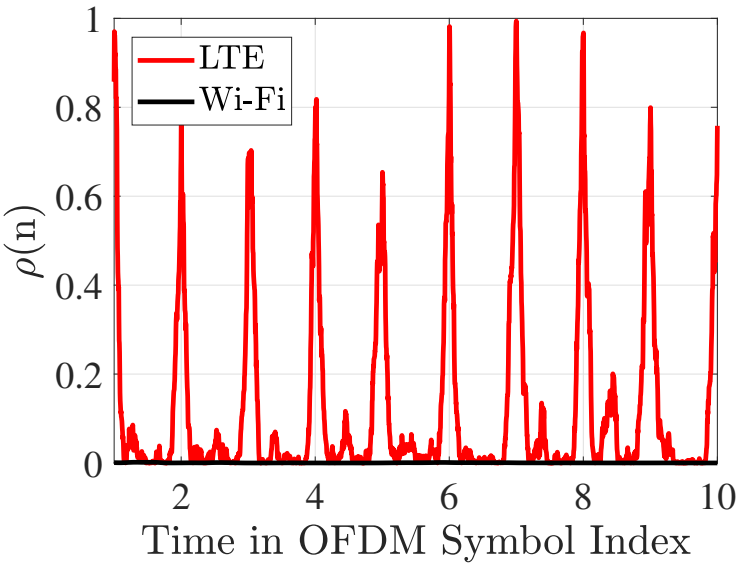

Figure 4.4: ρ(n) vs. n/(N+L).

for both LTE and Wi-Fi signals. The probability of false alarm rate P_{fa} is calculated by tracking the Wi-Fi OFDM symbols that are wrongly determined as LTE OFDM symbols when N = 320 and L = 64. This happens when $\rho(n)$ is calculated to be greater than the identification threshold. In Figure. 4.5(a), we plot P_d and P_{fa} as functions of the threshold used to identify the LTE transmissions. Intuitively, a larger threshold would lower the false alarm rate but will decrease the detection probability. We observe that with the same window size L and separation length N, P_{fa} is close to 0 irrespective of the threshold, meanwhile P_d is close to one if the threshold is less than 0.4. This indicates that it is practical and accurate to differentiate LTE signals from Wi-Fi signals.

In the third experiment, we investigated the effect of the distance between the LTE station and Wi-Fi terminal. We repeated the first two experiments but re-configured Wi-Fi to move away from the LTE station. In Figure. 4.5(b), we show P_d and P_{fa} as a function of the received power level at the Wi-Fi terminal. We control the amount of received power by controlling the distance d separating the two USRP devices. The identification threshold is set to 0.4. We see that, within

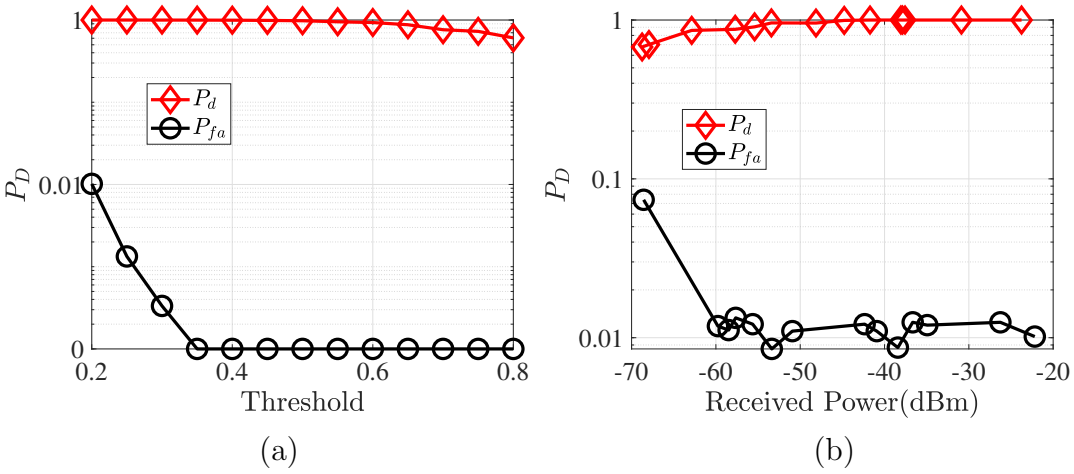

Figure 4.5: Detecting LTE signals: (a) Detection probability P_d as a function of the threshold and (b) Detection probability P_d as a function of the input power at Wi-Fi AP when the threshold is fixed.

the effective sensitivity range of Wi-Fi, we have a considerable detection probability even for low levels of detected power. Perfect detection conditions can be observed when the received power is greater than -45 dBm. Moreover, irrespective of the received power at Wi-Fi terminal, the false alarm rate is always around zero.

4.4.3 Differentiating between LTE Stations

We further performed a different set of experiments to evaluate the distinguishability technique between different LTE IDs. In this set of experiments, instead of considering OFDM symbols, we transmitted whole LTE frames including the secondary synchronization signal (SSS) and the primary synchronization signal (PSS). SSS and PSS are mapped to the last two OFDM symbols in first and sixth slots, as shown in Figure. 4.2. The correlation $\rho_{ID}(n)$ is calculated using a total of 640 samples, which is equal to the combined length of the two OFDM symbols carrying SSS and PSS. The two USRP devices were synchronized, thus the fifth and sixth OFDM symbols in each received frame is considered the SSS and PSS in our experiments, respectively. In the first part of the experiment, we transmitted LTE frames with the same SSS and PSS to evaluate the detection probability, then we transmit-

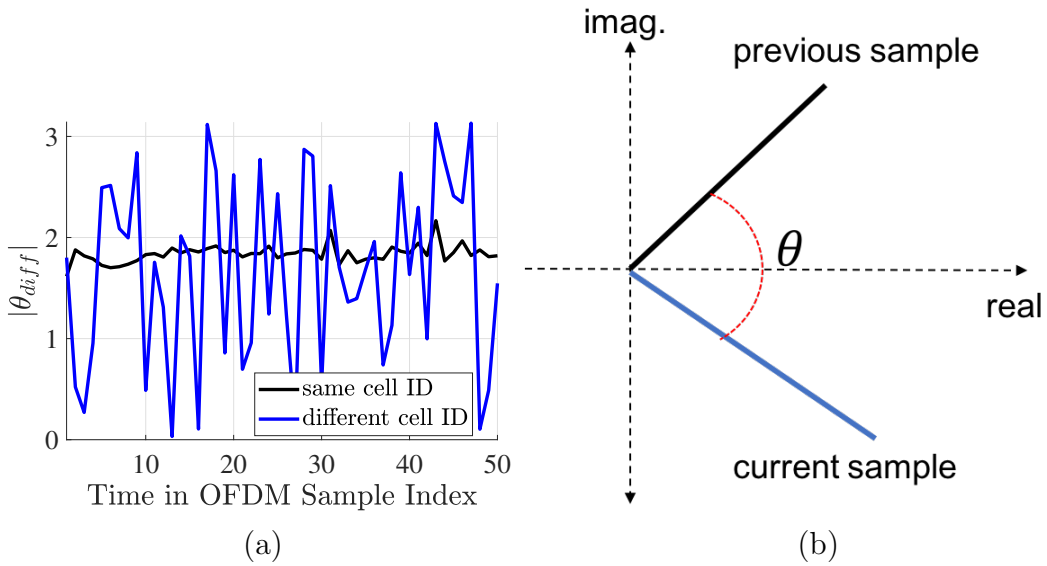

Figure 4.6: Carrier frequency offset in differentiating LTE transmissions: (a) Phase difference θ_{diff} as a function of time in OFDM sample index and (b) Carrier frequency offset between the previous sample and current sample.

ted LTE frames with different SSS and PSS to evaluate the false alarm probability. Due to the limited number of root indices of PSS, we also evaluated the case when the PSS is reused with different SSS'sand. Since our USRP devices can only send at most 320 frames in one experiment, we repeated each of these experiments 10 times in the sake of more accurate results, which means 3200 frames for this set of experiments.

During the experiment, we noticed from the collected data that a phase offset always existed among samples that belonged to consecutive frames. Figure 4.6(a) shows the absolute phase difference $|\theta_{diff}|$ between the samples carrying the PSS and SSS in two consecutive frames as a function of the OFDM sample index when 15 OFDM samples are detected. We see that $|\theta_{diff}|$ is almost constant when the same LTE ID is carried by the two frames, however this does not hold when different LTE ID is used. Figure 4.6(b) shows the phase and magnitude of two identical LTE samples, one from the previous received frame and the other is the corresponding one in the current frame. We see that both have the same magnitude but the phase is shifted due to the channel interference. To improve our identification method,

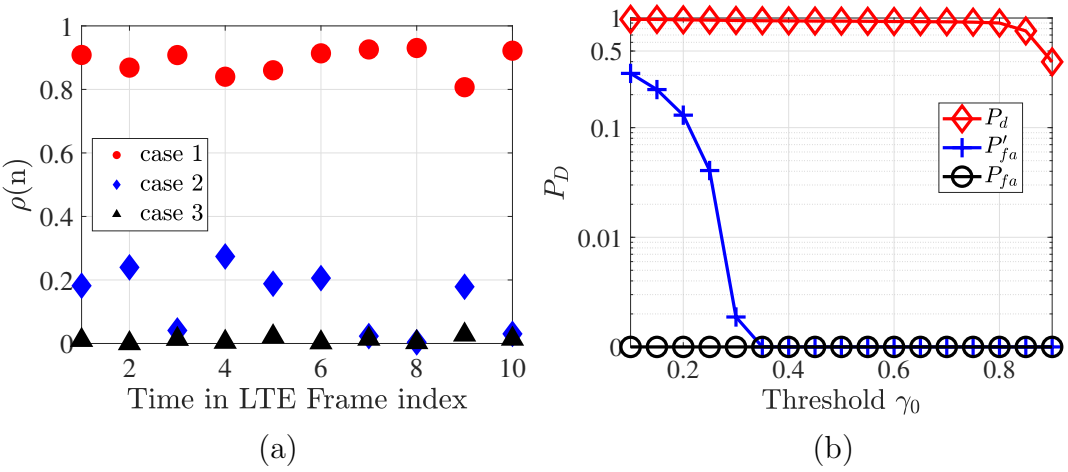

Figure 4.7: Differentiating LTE stations: (a) Correlation ρ(n) as a function of time in LTE frame index for cell ID distinguishability and (b) Detection probability P_d as a function of the threshold γ_0.

we applied a compensation technique on the phase parts of samples belong to two consecutive frames as follows

- We extract the samples of SSS and PSS of the current LTE frame and denote their phase part as s^{θ}_{ID}.
- The Wi-Fi terminal calculates the mean value σ of the difference between s^{θ}_{ID} and the phase part of the i^{th} LTE signature $s^{\theta}_{ID_i}$.
- The compensated phase part of the current frame's SSS and PSS is calculated as $s^{\theta'}_{ID} = (s^{\theta}_{ID} + \sigma) \bmod \pi$.
- ρ_{ID} is calculated between $s^{\theta}_{ID_i}$ and $s^{\theta'}_{ID}$ using equation (4.5).

We emphasize that this compensation method does not require the decodability of LTE transmissions. Intuitively, ρ_{ID} remains the same after compensation if the current frame carries different station PSS and SSS from s_{ID_i}, otherwise ρ_{ID} can be significantly increased. Figure. 4.7(a) shows ρ_{ID} as a function of the LTE frame index, when ten LTE transmissions are detected. We studied three different cases, all frames have: (1) Same PSS and SSS, (2) Same PSS and different SSS, and (3)

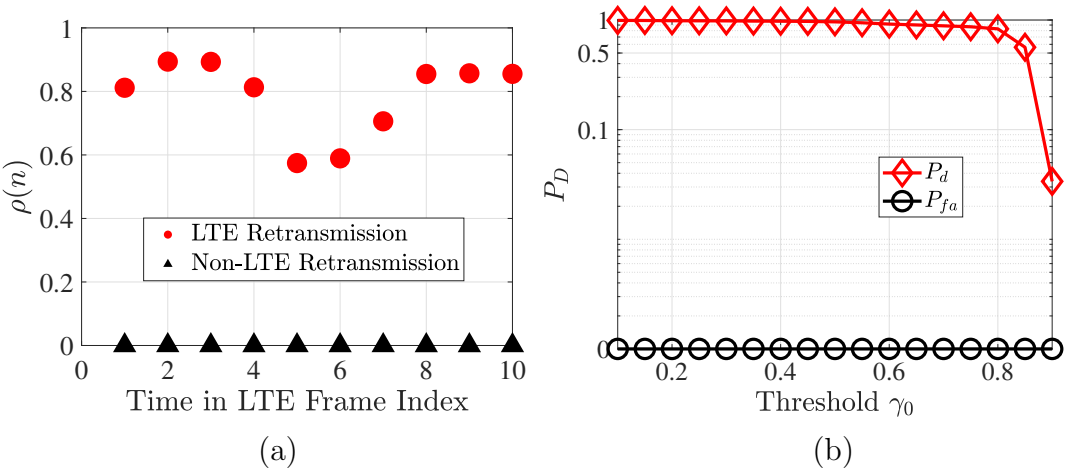

Figure 4.8: Detecting the retransmission round: (a) Correlation $\rho(n)$ as a function of time in LTE frame index for Retransmission detection and (b) Detection probability P_d as a function of the threshold γ_0.

Different PSS and SSS. For the first case, we always have a high correlation as all frames belong to the same LTE. For the second and third cases, frames belong to different LTE stations, thus the correlation is much lower. In Figure. 4.7(b), we plot the detection and false alarm probability for this experiment. The detection probability P_d denotes the correct estimation when LTE transmissions with the same PSS and SSS attributed to the same LTE station. The false alarm rate $P_{fa'}$ represents that LTE transmissions with the same PSS but different SSS are attributed to the same LTE station, while P_{fa} represents that LTE transmissions with different PSS and SSS are attributed to the same LTE station. As expected, P_{fa} is seen to be almost zero irrespective to the threshold. Whereas, $P_{fa}{}'$ can take non zero values, however choosing the threshold to be greater than 0.3 can force it to approach zero. Meanwhile, the scheme gives perfect detection if the threshold is less than 0.8. Our results justify the selection of the threshold to be in the range of $\gamma_0 \in [0.35, 0.8]$.

4.4.4 Identification of the Transmission Round

In the final set of experiments, we evaluated the estimation method for the transmission round. We assumed that the entire frame remains the same in each re-

transmission. So, we evaluated the similarity among frames. We used a correlation window of 38400 samples, which is the length of one LTE frame. The compensation mechanism used in the previous experiment is also introduced here but for the entire frame. Figure. 4.8(a) shows the correlation as a function of the LTE frame index when 10 frames are detected. We note that if the ten frames are retransmissions of the same frame, the correlation is high because of the similarity. However, if a new frame is transmitted each time the correlation is almost zero. In Figure. 4.8(b), we show P_d and P_{fa} for this scheme, as a function of the threshold γ_0. P_{fa} is evaluated by transmitting a new frame each time. We observe that P_{fa} is always close to zero, whereas P_d can be perfect if we choose the detection threshold to be around 0.1.

CHAPTER 5

IDLE SLOTS ESTIMATION AND PRIORITY CLASS ESTIMATION

In this chapter, we propose the power-saving mechanisms for energy-efficient LTE Wi-Fi coexistence built upon the implicit techniques in Chapter 4. We first discuss the idle slots estimation between two consecutive transmissions from the same LTE station. Then, we introduce two priority class estimation techniques to predict the used priority class of current LTE transmission.

5.1 Estimating Idle Slots

Consider the $(i-1)^{st}$ and i^{th} successive transmission of an LTE station A, as shown in Figure. 5.1. Let ν_i be the number of transmissions that belong to other terminals occurring before LTE A is able to transmit the i^{th} frame. Let also T_j be the idle time, in slots, between the $(j-1)^{th}$ and j^{th} intermediate transmission. The total

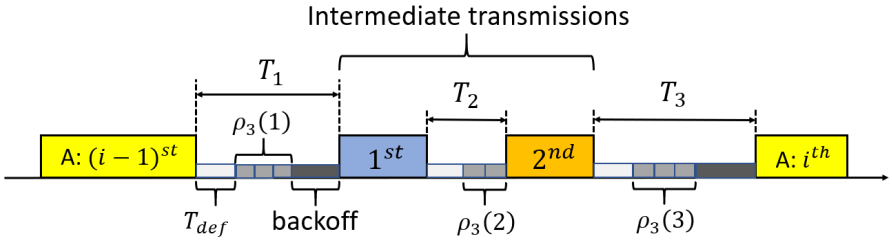

Figure 5.1: Elapsed time between two successive transmissions.

number of idle slots $\hat{N}(i)$ in the i^{th} backoff period is,

$$\hat{N}(i) = \sum_{j=1}^{\nu_i+1} T_j. \tag{5.1}$$

Note that T_j's are measured in slots. Wi-Fi X can also express $\hat{N}(i)$ for each priority class C_ℓ as

$$N_\ell(i) = B_\ell(i) + (\nu_i + 1)T_{def} + \sum_{j=1}^{\nu_i+1} \rho(j), \tag{5.2}$$

where $B_\ell(i)$ denotes the number of backoff slots for the i^{th} backoff period, T_{def} is the fixed defer period after every transmission and $\rho_\ell(j)$ accounts for the additional observation slots within T_j. The value for $\rho_\ell(j)$ is computed as follows:

$$\rho_\ell(j) = \begin{cases} \min\{\rho_\ell, T_j - T_{def}\}, & 1 \leq j \leq \nu_i, \\ \rho_\ell, & j = \nu_i + 1. \end{cases} \tag{5.3}$$

In (5.3), we have taken into account that a transmission from another LTE station or Wi-Fi terminal can start before the ρ_ℓ observation slots are over. To demonstrate the relationships in (5.1), (5.2), and (5.3), we consider the example in Figure 5.1, where the i^{th} frame of LTE A is of class C_3. The total elapsed idle slots between the $(i-1)^{st}$ and i^{th} transmission of A is $\hat{N}(i) = T_1 + T_2 + T_3$. According to (5.2), $\hat{N}(i)$ can be expressed as

$$N_3(i) = B_3(i) + 3T_{def} + \rho_3(1) + \rho_3(2) + \rho_3(3). \tag{5.4}$$

In this realization, A is in its backoff stage when the 1^{st} intermediate transmission starts and hence $\rho_3(1) = \rho_3 = 3$ slots, whereas the second transmission starts before A completes three observation slots and hence $\rho_3(2) = T_2 - T_{def} = 2$ slots. For the final set of elapsed idle slots, $\rho_3(3) = \rho_3 = 3$ slots because A must have backed off for the three slots designated by a C_3 transmission before it captures the medium. The backoff counter $B_3(i)$ is chosen uniformly from $[0, 15]$.

5.2 Priority Class Estimation

In this Section, we utilize the estimation of the parameter $\hat{N}(i)$ to infer the used priority class in the i^{th} transmission. From the number of intermediate transmissions ν_i, Wi-Fi X can use the relationship in (5.2) to compute the range of the elapsed idle slots $N_\ell(i)$ given the class C_ℓ. The range is given by $N_\ell(i) \in [N_\ell^{\min}(i), N_\ell^{\max}(i)]$ where

$$N_\ell^{\min}(i) = (\nu_i + 1)T_{def} + \sum_{j=1}^{\nu_i+1} \rho_\ell(j), \tag{5.5}$$

$$N_\ell^{\max}(i) = (q_{min} - 1) + (\nu_i + 1)T_{def} + \sum_{j=1}^{\nu_i+1} \rho_\ell(j), \tag{5.6}$$

where the minimum and maximum possible backoff counters are zero and $(q_{min} - 1)$, respectively.

The range of $N_\ell(i)$ together with its estimate from (5.1) enable Wi-Fi terminal X to identify the possible priority classes for the i^{th} transmission as follows:

1. Between the $(i-1)^{st}$ and i^{th} transmission of an LTE A, Wi-Fi X records ν_i and T_j and estimates $\hat{N}(i)$ using (5.1).

2. Using ν_i, Wi-Fi X computes the elapsed idle slot range $[N_\ell^{\min}(i), N_\ell^{\max}(i)]$ for each class C_ℓ.

3. Wi-Fi X constructs a binary vector $\mathbf{I}_C(i) = (I_1, I_2, I_3, I_4)$ where $I_\ell = 1$, if $\hat{N}(i) \in [N_\ell^{\min}(i), N_\ell^{\max}(i)]$ and zero otherwise.

4. In case that Wi-Fi X oversleeps or collision happens, the vector is set to $\mathbf{I}_C(i) = (1, 1, 1, 1)$, i.e., all classes are possible.

The vector $\mathbf{I}_C(i)$ denotes the set of possible priority classes for the i^{th} transmission that can yield the estimated number of idle slots $\hat{N}(i)$. If the vector's cardinality is

$|\mathbf{I}_C(i)| = 1$, then the priority class of the i^{th} transmission is identified with certainty. However, in most cases, it is expected that $|\mathbf{I}_C(i)| > 1$. In the latter case, we introduce two mechanisms for priority class estimation. The transmit-first approach prevents any oversleeping by the Wi-Fi whereas in the second approach, we apply Bayesian estimation to best estimate the priority class.

5.2.1 The Transmit-First Class Estimation

In the first approach, the Wi-Fi terminal selects the highest priority class C_ℓ from set $\mathbf{I}_C(i)$ for which $I_\ell(i) = 1$. The higher priority classes have a shorter channel occupancy time T_ℓ^{MCOP}, leading to a shorter dwelling in sleep mode. This conservative approach allows the Wi-Fi terminal to return to idle mode just before the LTE transmission has ended and continue to contend for the channel. Thus, it prevents any missed transmission opportunities due to false class estimation and oversleeping. This comes at the expense of a lower energy savings when the class of a frame is falsely estimated.

As an example, assume that based on $\hat{N}(i)$, the Wi-Fi estimates vector $\mathbf{I}_C(i) = \{0, 1, 1, 0\}$, i.e, the possible classes for the eminent i^{th} LTE transmission are either C_2 with $T_2^{MCOP} = 3$ms, or C_3 with $T_3^{MCOP} = 8$ms. If the Wi-Fi selected C_3 and stayed in sleep mode for 8ms, but a C_2 frame was transmitted, the Wi-Fi would miss the opportunity to contend after the first 3ms. Under the transmit-first approach, the Wi-Fi always chooses the highest class (C_2 in this case), and therefore sleeps for 3ms. This guarantees that given the candidate classes, the WI-Fi will not oversleep. On the other hand, when C_2 is selected by a C_3 frame is transmitted, the Wi-Fi loses the opportunity to stay in sleep mode for an additional 5ms. The rationale here is that performance in terms of throughput gets a higher priority to energy savings. One of the possible improvement of the Transmit-First Class estimation is to sleep again when terminal wakes up and learns that it wakes up earlier. The problem is, even though the power consumption and transition time from idle mode to sleep mode is negligible, the power consumption during switching time of wakeup

is equal to the power consumption on active mode [40]. In [41], the switching time from sleep mode to active mode is 2 ms. Based on 802.11 standard [42], the time required to receive a Beacon Frame is about 1 ms, which means the switching time from sleep mode to active mode is 1 ms. In addition, it is reasonable to assume that new chipsets could achieve further reduction on this switching time. Meanwhile, our work assumes Wi-Fi terminals switch from sleep mode to idle mode, instead of active mode, which can be even lower.

5.2.2 Bayes-based Estimation

In the second approach, the Wi-Fi estimates the priority class of the i^{th} LTE transmission using the knowledge of $\hat{N}(i)$ and the empirical priority class distribution based on prior transmission history. Specifically, we employ Bayesian estimation to compute the posterior class probabilities given the observation $\hat{N}(i)$. Formally, the estimated class $C_\ell^*(i)$ for the i^{th} transmission is determined by.

$$\begin{aligned} C_\ell^*(i) &= \underset{C_\ell \in \{C_1, C_2, C_3, C_4\}}{\operatorname{argmax}} P(C_\ell | \hat{N}(i)) \\ &= \underset{C_\ell \in \{C_1, C_2, C_3, C_4\}}{\operatorname{argmax}} \frac{P(C_\ell) P(\hat{N}(i) | C_\ell)}{P(\hat{N}(i))}. \end{aligned} \tag{5.7}$$

In (5.7), the conditional probability $P(\hat{N}(i)|C_\ell)$ can be computed based on the backoff counter $B_\ell(i)$. For a class C_ℓ for which $I_\ell = 1$, i.e., $\hat{N}(i)$ is within the expected idle slot range of that class. the backoff counter $B_\ell(i)$ can be computed by setting $N_\ell(i) = \hat{N}(i)$ and solving for $B_\ell(i)$ (both ν_i and $\rho_\ell(j), \forall j$ are observable and fixed in the i^{th} realization). Given that $B_\ell(i)$ is uniformly selected from $[0, q_\ell(i) - 1]$, where $q_\ell(i)$ denotes the contention window size for the i^{th} transmission, it follows that

$$P(\hat{N}(i)|C_\ell) = P(B_\ell(i)|C_\ell) = \frac{1}{q_\ell(i) - 1}. \tag{5.8}$$

If $I_\ell = 0$, i.e., an LTE frame of class C_ℓ is not feasible for the observed $\hat{N}(i)$, then $P(\hat{N}(i)|C_\ell) = 0$. The two cases can be summarized to

$$P(\hat{N}(i)|C_\ell) = \frac{I_\ell(i)}{q_\ell(i) - 1}. \tag{5.9}$$

To build the likelihood prior of $P(C_\ell)$, we use the sample relative frequencies obtained from the history of the LTE transmissions. Here, we do not apply any smoothing via a kernel density estimation process [43] because of the small number of classes (four in total) and relatively large number of observations. We do, however, adjust for recent history to capture the temporal correlation of LTE transmissions. We expect that recent history reflects more accurately the probability of observing a frame that belongs to a specific class. For instance, a video transmission involves a sequence of frames that belong to C_3 or C_4, thus temporarily skewing the pmf. To account for recent history, we calculate $P(C_\ell)$ as the weighted average of the relative sample frequencies over two time scales.

$$P(C_\ell) = \alpha(i)\frac{n'_\ell}{n'} + (1 - \alpha(i))\frac{n_\ell}{n}, \tag{5.10}$$

where ${}^{n'_\ell}/_{n'}$ is the relative sample frequency of C_ℓ over the n' most recent observations, ${}^{n_\ell}/_{n}$ is the relative sample frequency of C_ℓ over all n observations, and $\alpha(i)$ is a weight factor that is optimized after every transmission is completed.

Determination of $\alpha(i)$: The weighting factor $\alpha(i)$ can be continuously optimized to minimize the mean square error (MSE) of the class estimator. Here, we utilize the fact that the Wi-Fi can infer the actual LTE class at the end of each LTE transmission upon its completion. Let $H_\ell(i)$ indicate the actual priority class that the Wi-Fi inferred at the end of i^{th} transmission, i.e., $H_\ell(i) = 1$ if the LTE use C_ℓ. The MSE is given by

$$MSE(i) = \frac{1}{4}\sum_{\ell=1}^{4}(P(C_\ell) - H_\ell(i))^2. \tag{5.11}$$

where $P(C_\ell)$ denotes the estimated probability of priority class C_ℓ for the i^{th} transmission. Substituting $P(C_\ell)$ with (5.10), yields

$$MSE(i) = \frac{1}{4}\sum_{\ell=1}^{4}\left(\left(\frac{n'_\ell}{n'} - \frac{n_\ell}{n}\right)\alpha(i) + \left(\frac{n_\ell}{n} - H_\ell(i)\right)\right)^2, \quad (5.12)$$

To minimize $MSE(i)$, we differentiate with respect to α

$$\frac{d(MSE(i))}{d\alpha} = \frac{1}{2}\sum_{\ell=1}^{4}\left(\left(\frac{n'_\ell}{n'} - \frac{n_\ell}{n}\right)^2\alpha(i) + \left(\frac{n'_\ell}{n'} - \frac{n_\ell}{n}\right)\left(\frac{n_\ell}{n} - H_\ell(i)\right)\right). \quad (5.13)$$

Solving $\frac{d(MSE(i))}{d\alpha} = 0$ yields

$$\alpha(i) = \frac{\sum_{\ell=1}^{4}\left(\frac{n'_\ell}{n'} - \frac{n_\ell}{n}\right)\left(H_\ell(i) - \frac{n'_\ell}{n}\right)}{\sum_{\ell=1}^{4}\left(\frac{n'_\ell}{n'} - \frac{n_\ell}{n})^2\right)}. \quad (5.14)$$

The updated value $\alpha(i)$, evaluated by minimizing the MSE at the i^{th} transmission is used for estimating priority class of the $(i+1)^{th}$ transmission. Finally, the Wi-Fi computes $P(\hat{N}(i))$ as

$$P(\hat{N}(i)) = \sum_{\ell=1}^{4} P(C_\ell)\cdot P(\hat{N}(i)|C_\ell), \quad (5.15)$$

where $P(C_\ell)$ is given in (5.10) and $P(\hat{N}(i)|C_\ell)$ is given in (5.9).

CHAPTER 6

PERFORMANCE EVALUATION

In this chapter, we evaluate the performance of the proposed power-saving mechanisms through simulations. We implemented an event-based simulation to evaluate the mechanisms proposed in Chapter 5. We used the class detection probability P_d, the probability of early wake up P_e, P_c the probability of missing channel contention chances due to late wake-up, and the ratio of time duration between sleeping time T_{sleep} and busy time T_{busy} to measure the performance of proposed mechanisms. Hence, we calculated the ratio between the power consumption with the use of the proposed mechanism and that without using any schemes.

We deployed three LTE stations and one Wi-Fi terminal in the same collision domain. All terminals were assumed to be backlogged. The LTE stations followed the LAA-LTE specification, whereas the Wi-Fi terminal implemented the IEEE 802.11ac protocol. We ran our simulations for 100,000 events, where each event represents one LTE transmission attempt. We considered three cases regarding the class distribution of LTE traffic. Case 1 includes predominately high priority traffic with the probability of each class being $\{0.45, 0.45, 0.05, 0.05\}$. Case 2 implements a scenario of predominately low priority traffic with probabilities $\{0.05, 0.05, 0.45, 0.45\}$. Finally, in case 3 all classes are equiprobable. Then, to capture the correlation among consecutive transmissions, we use normal distribution with mean μ and variance σ^2 to draw N_{μ,σ^2} the number of consecutive transmissions that follow the same class. We do not draw a new class until N_{μ,σ^2} packets are transmitted. For each case, we considered a high correlation scenario with $\mu = 10$ and $\sigma^2 = 5$ and a low correlation scenario with $\mu = 1$ and $\sigma^2 = 1$. The key parameters of our evaluation are the correct T_ℓ^{MCOP} estimation probability P_d, the probability of an early wake up P_e due to wrongly estimating a higher priority class, and the probability of oversleeping

P_c due to wrongly estimating a lower priority class.

In the first set of experiments, we studied the high correlation scenario. Figure 6.1(a) shows P_d as a function of the length of the recent history n'. We observe that Bayes estimation yields over 95% estimation accuracy when $n' = 1$. This indicates that the class of the previous LTE transmission is the strongest indicator for the following LTE transmission. We further observe that when the majority of the traffic is either Class 3 or Class 4 (case 2), the estimation is more accurate because it easier to distinguish between $\{C_1, C_2\}$ and $\{C_3, C_4\}$ due to their large difference in ρ_ℓ. Finally, we show the performance of the transmit-first strategy ($n' = 0$). Although this strategy does not take into account the prior history, it performs acceptably in estimating the traffic class solely based on the $\hat{N}(i)$ range.

In Fig. 6.1(b), and Fig. 6.1(c), we show the impact of erroneous class estimation on the energy conservation and the loss of transmission opportunities. We observe that the majority of the false estimation $(1 - P_d)$ results in early wake (P_e) up for cases 1 and 3 and is almost equally divided for case 2. The higher percentage of early wake ups is justified by the difference in T_ℓ^{MCOP} between the classes. When a lower priority class (classes 3 and 4) are misclassified, this leads to an early wake up. However, when a higher priority class is misclassified that does not necessarily lead to oversleeping because $T_3^{MCOP} = T_4^{MCOP}$. Moreover, in Fig. 6.1(c), we observe that the transmit-first approach ($n' = 0$) has a zero oversleeping probability due to the selection of highest priority class (lowest T_ℓ^{MCOP}).

In Fig. 6.1(d), we study the ratio between the time slept by the Wi-Fi (T_S) and the actual time that the channel is occupied (T_{busy}) by the LTE. As expected from Fig. 6.1(a-c), $n' = 1$ yields the best sleeping strategy. We also observe reverse trends in this ratio for the different class distributions as a function of n'. The distribution that favors higher classes (case 2) stays closer to the true busy state of LTE, but tends to oversleep, whereas in the other two cases, early wake-up is the most likely scenario as n' increases.

We repeated the first set of experiments for the low correlation scenario ($\mu = 1$

and $\sigma^2 = 1$). Fig. 6.2 shows a decreased detection performance relative to the results for the high correlation scenario (Fig. 6.1). This occurs because the LTE frame class changes rapidly leading to more frequent errors in estimation. The trends in early wake ups and oversleeping remain the same for the three class distributions.

We further evaluated the energy efficiency achieved by our proposed mechanism by computing the ratio of the energy consumed when the Wi-Fi goes to sleep during the LTE transmission denoted by E_C over the energy consumed when the current protocols are executed, denoted by E_T. We assumed that the Wi-Fi AP operates on priority class 1 with $T_\ell^{MCOP} = 1.504ms$. Both E_C and E_T are calculated from (3.1), with $P_A = 1.687$W, $P_I = 1.038$W and $P_S = 0.088$W [10]. Figures 6.3(a) and 6.3(b) shows over 60% energy savings (lower ratio is better) for both the Bayes estimation and transmit-first mechanisms. As expected, the Bayes estimation with $n' = 1$ achieves the best performance for all cases. Moreover, the transmit-first approach achieves significant savings without sacrificing any transmission opportunities for the Wi-Fi, as it never leads to oversleeping.

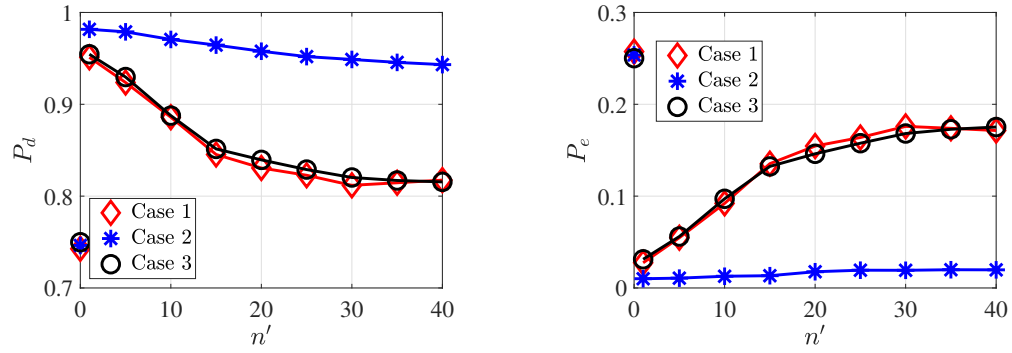

(a) P_d.

(b) P_e.

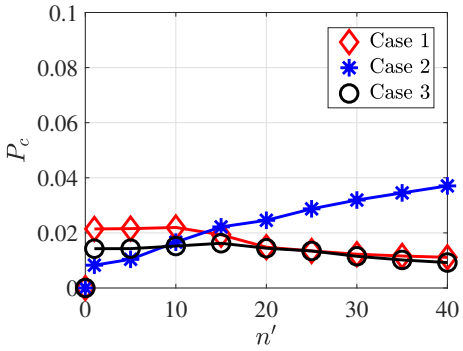

(c) P_c.

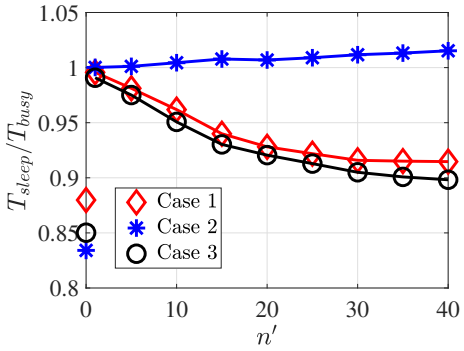

(d) T_{sleep}/T_{busy}.

Figure 6.1: Estimation performance for the high correlation scenario ($\mu = 10$ and $\sigma^2 = 5$) as a function of the history length n'.

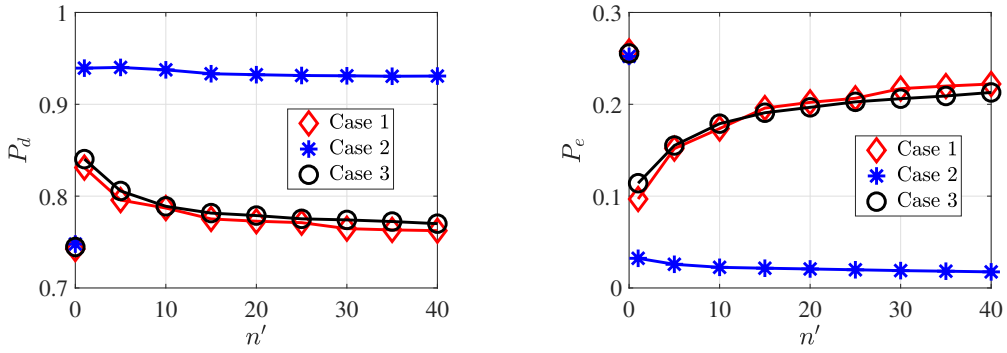

(a) P_d.

(b) P_e.

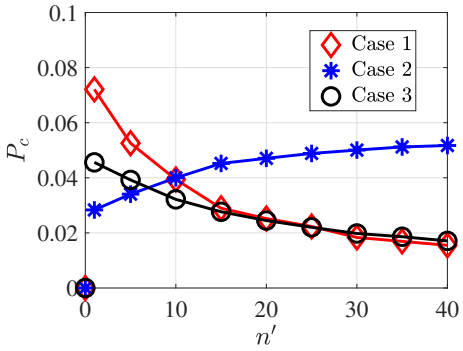

(c) P_c.

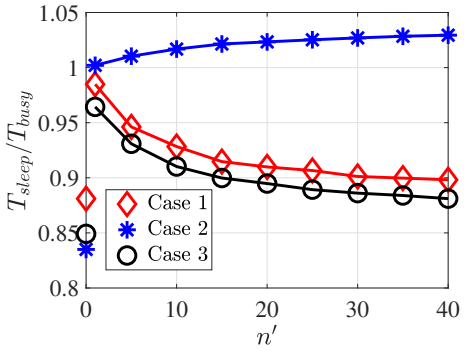

(d) T_{sleep}/T_{busy}.

Figure 6.2: Estimation performance for the low correlation scenario ($\mu = 1$ and $\sigma^2 = 1$) as a function of the history length n'.

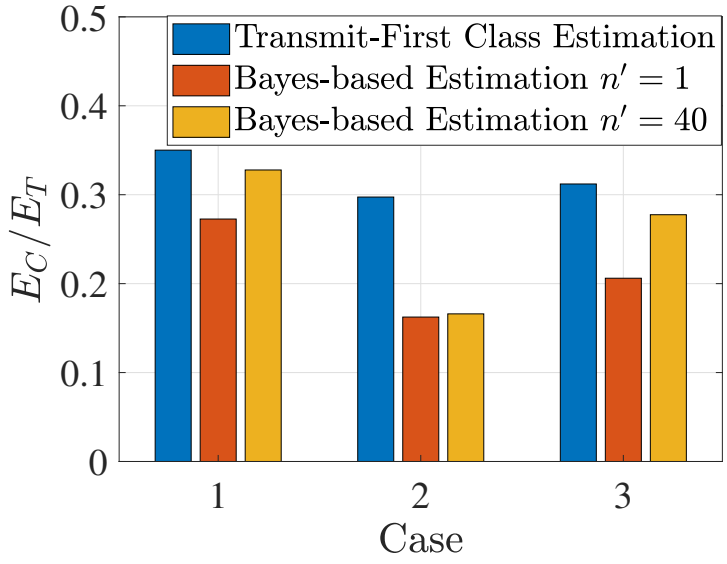

(a) With $\mu = 10$.

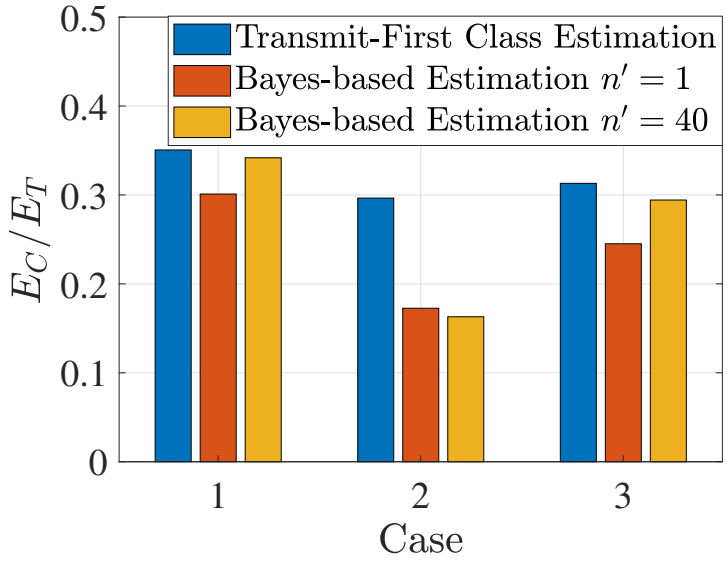

(b) With $\mu = 1$.

Figure 6.3: E_C/E_T for the different cases.

CHAPTER 7

SUMMARY OF CONTRIBUTIONS AND FUTURE RESEARCH DIRECTIONS

7.1 Summary of Contributions

Although the heterogeneous systems coexistence regarding the channel contention unfairness has been a subject of research in recent years, the power consumption among heterogeneous technologies has received little attention. The LTE/Wi-Fi coexistence without explicit coordination messages can cause considerable power consumption, especially, on Wi-Fi AP side as the most Wi-Fi devices are battery-powered. In this thesis, We studied the problem of energy efficiency under LAA-LTE/Wi-Fi coexistence in unlicensed bands. We presented a new method for achieving implicit coordination between coexisting Wi-Fi and LTE systems. Our goal was to enable terminals transition to sleep mode when other terminals transmitted. We proposed a mechanism that enable Wi-Fi terminals to estimate the priority class of an imminent LTE transmission by analyzing the elapsed idle slots between two consecutive transmissions from the same LTE station and the prior transmission history. We show that our method leads to over 60% in energy savings in various traffic scenarios. Although we presented our method from the perspective of the Wi-Fi terminal, the same estimation approach can be adopted by LTE stations to be set to sleep mode during Wi-Fi transmission.

Meanwhile, we proposed and evaluated two implicit techniques that enable Wi-Fi AP to detect LTE signals and differentiate LTE transmissions from different LTE stations without decoding the LTE signals. We performed experiments using NI-USRP 2921 devices to simulate LTE/Wi-Fi coexistence. We show that the LTE detection probability is almost 1 and the false alarm rate is close 0 when the AP

implements CP-based scheme with the threshold less than 0.4. In addition, we show that, by correlating the LTE cell ID (PSS and SSS), the AP can yield almost 100% detection probability with false alarm rate is close to 0 when the AP differentiates LTE transmissions with the selection of the threshold within the range of $\gamma_0 \in [0.35, 0.8]$.

REFERENCES

[1] FCC. Second memorandum opinion and order: In the matter of unlicensed operation in the tv broadcast band and additional spectrum for unlicensed devices below 900 mhz in the 3 ghz band. https://apps.fcc.gov/edocs_public/attachmatch/FCC-08-260A1.pdf, 2010.

[2] Qualcomm. Qualcomm whitepaper: Extending lte advanced to unlicensed spectrum. https://www.qualcomm.com/media/documents/files/white-paper-extending-lte-advanced-to-unlicensed-spectrum.pdf, 2013.

[3] 3GPP. Tr 36.889: Feasibility study on licensed-assisted access to unlicensed spectrum. https://portal.3gpp.org/desktopmodules/Specifications/SpecificationDetails.aspx?specificationId=2579, 2015.

[4] FCC. Fcc 16-89: Use of spectrum bands above 24 ghz for mobile radio services, et al. https://apps.fcc.gov/edocs_public/attachmatch/FCC-16-89A1_Rcd.pdf, 2016.

[5] Qualcomm. Lte in unlicensed spectrum: Harmonious coexistence with wi-fi. 2014.

[6] 3GPP TS 36.213 version 15.2.0 Release 15. Lte; evolved universal terrestrial radio access (e-utra); physical layer procedures. 2018.

[7] M. Hirzallah, W. Afifi, and M. Krunz. Full-duplex spectrum sensing and fairness mechanisms for Wi-Fi/LTE-U coexistence. In *2016 IEEE Global Communications Conference (GLOBECOM)*, pages 1–6, Dec 2016.

[8] Islam Samy, Loukas Lazos, Yong Xiao, Ming Li, and Marwan Krunz. Lte misbehavior detection in wi-fi/lte coexistence under the laa-lte standard. In *Proceedings of the 11th ACM Conference on Security & Privacy in Wireless and Mobile Networks*, WiSec '18, pages 87–98. ACM, 2018.

[9] IEEE Standard for Information technology Telecommunications and information exchange between systems Local and metropolitan area networks—Specific requirements - Part 11: Wireless LAN Medium Access Control (MAC) and Physical Layer (PHY) Specifications. *IEEE Std 802.11 (Revision of IEEE Std 802.11-2012)*, Dec 2016.

[10] Y. Xiao, Y. Cui, P. Savolainen, M. Siekkinen, A. Wang, L. Yang, A. Ylä-Jääski, and S. Tarkoma. Modeling energy consumption of data transmission over wi-fi. *IEEE Transactions on Mobile Computing*, 13(8):1760–1773, Aug 2014.

[11] 3GPP TS 36.213 version 10.1.0 Release 10. Lte; evolved universal terrestrial radio access (e-utra); physical layer procedures. 2011.

[12] 3GPP TS 36.213 version 11.0.0 Release 11. Lte; evolved universal terrestrial radio access (e-utra); physical layer procedures. 2012.

[13] S. Sagari, S. Baysting, D. Saha, I. Seskar, W. Trappe, and D. Raychaudhuri. Coordinated dynamic spectrum management of LTE-U and Wi-Fi networks. In *2015 IEEE International Symposium on Dynamic Spectrum Access Networks (DySPAN)*, pages 209–220, Sep. 2015.

[14] M. Hirzallah, W. Afifi, and M. Krunz. Full-duplex-based rate/mode adaptation strategies for wi-fi/lte-u coexistence: A pomdp approach. *IEEE Journal on Selected Areas in Communications*, 35(1):20–29, Jan 2017.

[15] Islam Samy and Loukas Lazos. Optimum priority class selection under wi-fi/lte coexistence. 04 2019.

[16] R. Ratasuk, M. A. Uusitalo, N. Mangalvedhe, A. Sorri, S. Iraji, C. Wijting, and A. Ghosh. License-exempt LTE deployment in heterogeneous network. In *2012 International Symposium on Wireless Communication Systems (ISWCS)*, pages 246–250, Aug 2012.

[17] Cristina Cano, Douglas J Leith, Andres Garcia-Saavedra, and Pablo Serrano. Fair coexistence of scheduled and random access wireless networks: Unlicensed lte/wifi. *IEEE/ACM Transactions on Networking*, 25(6):3267–3281, 2017.

[18] R. Yin, G. Yu, A. Maaref, and G. Y. Li. Lbt-based adaptive channel access for lte-u systems. *IEEE Transactions on Wireless Communications*, 15(10):6585–6597, Oct 2016.

[19] Michael Buettner, Gary V. Yee, Eric Anderson, and Richard Han. X-mac: A short preamble mac protocol for duty-cycled wireless sensor networks. In *Proceedings of the 4th International Conference on Embedded Networked Sensor Systems*, SenSys '06, pages 307–320, New York, NY, USA, 2006. ACM.

[20] R. C. Carrano, D. Passos, L. C. S. Magalhaes, and C. V. N. Albuquerque. Survey and taxonomy of duty cycling mechanisms in wireless sensor networks. *IEEE Communications Surveys Tutorials*, 16(1):181–194, First 2014.

[21] K. Han, J. Luo, Y. Liu, and A. V. Vasilakos. Algorithm design for data communications in duty-cycled wireless sensor networks: A survey. *IEEE Communications Magazine*, 51(7):107–113, July 2013.

[22] Yanjun Sun, Omer Gurewitz, and David B. Johnson. Ri-mac: A receiver-initiated asynchronous duty cycle mac protocol for dynamic traffic loads in wireless sensor networks. In *Proceedings of the 6th ACM Conference on Embedded Network Sensor Systems*, SenSys '08, pages 1–14, New York, NY, USA, 2008. ACM.

[23] C. M. Vigorito, D. Ganesan, and A. G. Barto. Adaptive control of duty cycling in energy-harvesting wireless sensor networks. In *2007 4th Annual IEEE Communications Society Conference on Sensor, Mesh and Ad Hoc Communications and Networks*, pages 21–30, June 2007.

[24] C. C. Enz, A. El-Hoiydi, J. . Decotignie, and V. Peiris. Wisenet: an ultralow-power wireless sensor network solution. *Computer*, 37(8):62–70, Aug 2004.

[25] Yanjun Sun, Omer Gurewitz, Shu Du, Lei Tang, and David B. Johnson. Adb: An efficient multihop broadcast protocol based on asynchronous duty-cycling in wireless sensor networks. In *Proceedings of the 7th ACM Conference on Embedded Networked Sensor Systems*, SenSys '09, pages 43–56, New York, NY, USA, 2009. ACM.

[26] P. Huang, L. Xiao, S. Soltani, M. W. Mutka, and N. Xi. The evolution of mac protocols in wireless sensor networks: A survey. *IEEE Communications Surveys Tutorials*, 15(1):101–120, First 2013.

[27] Giuseppe Anastasi, Marco Conti, Mario Di Francesco, and Andrea Passarella. Energy conservation in wireless sensor networks: A survey. *Ad Hoc Netw.*, 7(3):537–568, May 2009.

[28] Khaled Arisha, Moustafa Youssef, and Mohamed Younis. *Energy-Aware TDMA-Based MAC for Sensor Networks*, pages 21–40. Springer US, Boston, MA, 2002.

[29] Venkatesh Rajendran, Katia Obraczka, and J. J. Garcia-Luna-Aceves. Energy-efficient, collision-free medium access control for wireless sensor networks. *Wireless Networks*, 12(1):63–78, Feb 2006.

[30] W. R. Heinzelman, A. Chandrakasan, and H. Balakrishnan. Energy-efficient communication protocol for wireless microsensor networks. In *Proceedings of the 33rd Annual Hawaii International Conference on System Sciences*, pages 10 pp. vol.2–, 2000.

[31] L F. W. Van Hoesel and Paul Havinga. A lightweight medium access protocol (lmac) for wireless sensor networks. *INSS*, 01 2004.

[32] S. Chatterjea, L. F. W. van Hoesel, and P. J. M. Havinga. Ai-lmac: an adaptive, information-centric and lightweight mac protocol for wireless sensor networks. In *Proceedings of the 2004 Intelligent Sensors, Sensor Networks and Information Processing Conference, 2004.*, pages 381–388, Dec 2004.

[33] Joseph Polastre, Jason Hill, and David Culler. Versatile low power media access for wireless sensor networks. In *Proceedings of the 2Nd International Conference on Embedded Networked Sensor Systems*, SenSys '04, pages 95–107. ACM, 2004.

[34] Yu-Chee Tseng, Chih-Shun Hsu, and Ten-Yueng Hsieh. Power-saving protocols for ieee 802.11-based multi-hop ad hoc networks. In *Proceedings.Twenty-First Annual Joint Conference of the IEEE Computer and Communications Societies*, volume 1, June 2002.

[35] Wei Ye, J. Heidemann, and D. Estrin. Medium access control with coordinated adaptive sleeping for wireless sensor networks. *IEEE/ACM Transactions on Networking*, 12(3):493–506, June 2004.

[36] Mohammed Hirzallah, Wessam Afifi, and Marwan Krunz. Full-duplex spectrum sensing and fairness mechanisms for wi-fi/lte-u coexistence. In *Global Communications Conference (GLOBECOM), 2016 IEEE*, pages 1–6. IEEE, 2016.

[37] Shyamnath Gollakota and Dina Katabi. *Zigzag decoding: combating hidden terminals in wireless networks*, volume 38. ACM, 2008.

[38] Jim Zyren. Overview of the 3gpp long term evolution physical layer. 01 2007.

[39] Jan-Jaap Van de Beek, Magnus Sandell, and Per Ola Borjesson. Ml estimation of time and frequency offset in ofdm systems. *IEEE transactions on signal processing*, 45(7):1800–1805, 1997.

[40] G. Anastasi, M. Conti, E. Gregori, and A. Passarella. 802.11 power-saving mode for mobile computing in wi-fi hotspots: Limitations, enhancements and open issues. *Wirel. Netw.*, 14(6):745–768, December 2008.

[41] Ronny Krashinsky and Hari Balakrishnan. Minimizing energy for wireless web access with bounded slowdown. *Wireless Networks*, 11:135–148, 2005.

[42] IEEE Standard for Wireless LAN Medium Access Control (MAC) and Physical Layer (PHY) specifications. *IEEE Std 802.11-1997*, pages 1–445, Nov 1997.

[43] Silverman, B.W. Density estimation for statistics and data analysis. Chapman and Hall, `https://doi.org/10.1201/9781315140919`, 1986.